Optimisation of Strength and Ductility of Cu-Cr-Zr by Combining Severe Plastic Deformation and Precipitation

K. Valdés León, M.A. Muñoz-Morris and D.G. Morris*

Department of Physical Metallurgy, CENIM, CSIC, Avenida Gregorio del Amo 8, E-28040 Madrid, Spain

[* corresponding author. Tel +34-91-553-8900; fax: +34-91-534-7425;
E-mail address: david.morris@cenim.csic.es]

Abstract

The microstructure and mechanical behaviour of a Cu-Cr-Zr alloy has been examined after severe plastic deformation, and giving both prior and subsequent age hardening treatments. Dislocation subgrain structures are produced by deformation leading to high strength and reduced ductility. Mild annealing following deformation leads to slight substructural coarsening, some loss of dislocations, and simultaneous precipitation, resulting in an increase of strength with some improvement of ductility. The same heat treatments for precipitation before deformation lead to finer substructures, with shear reducing particle size and leading to partial dissolution. Strength and ductility are analysed in terms of the deformation substructures and the role of precipitate particles.

Keywords:

1. Introduction

Cu-Cr-Zr alloys are of great interest in the electric/microelectronic industries because of their high strength, retained to high temperatures, combined with good formability and good conductivity. Such properties also make these alloys interesting for several components in nuclear fusion reactors [1]. These materials are strengthened by cold

working, as well as by precipitation of Cr and complex Cu-Zr phases [1,2]. Precipitation and hardening in these alloys is well understood [1,2], following considerable work over many decades which has also looked at the role of prior plastic deformation on precipitation and strengthening, as well as the role of further alloying elements to the Cu-Cr or Cu-Cr-Zr base, including additions such as P,Mg [3,4].

Severe plastic deformation, often carried out by equal channel angular pressing (ECAP), has been examined extensively over the last decade in a wide range of ductile metals and alloys [5,6], including pure Cu [7,8] and Cu-Cr [9-11] and Cu-Cr-Zr [12] alloys. Microstructure is refined to equiaxed subgrains/grains about 100-200 nm in size when deforming to high strains, accompanied by a significant strength increase. Boundaries of relatively low misorientation are formed at low levels of strain, which are progressively converted to higher angle grain boundaries at higher strains [8,9]. The strengthening achieved has been interpreted as dislocation hardening [8] or dislocation cell wall hardening [7], with the transition from low to high angle subgrain/grain boundaries meaning that Hall-Petch grain size hardening becomes important at high strains [9-11]. At the same time the ductility remains good for such heavily deformed Cu alloys.

Several studies have examined the mechanical behaviour of Cu-Cr and Cu-Cr-Zr alloys which have received ageing-precipitation treatments either before [10] or after [11,12] ECAP. Ageing after ECAP led to accelerated precipitation as compared with the solutionised material [9,12], with an interesting increase in both strength and ductility observed in all cases [10-12], similar to increases after precipitation reported previously for roll-bonded Cu-Cr-Zr alloy [13] and for some ECAP-processed Al alloys [5,14,15].

The present study examines the strength and ductility of a Cu-Cr-Zr alloy processed by ECAP and then aged, or given an ageing treatment before ECAP. This allows a comparison of microstructural evolution and plastic deformation behaviour for both routes. It is, for example, possible to compare the evolution of microstructure during severe plastic deformation of solutionised material, which is subsequently aged, with that occurring in material already containing fine precipitates. The effect of nanoprecipitates on mechanical behaviour may thus be distinguished from that due to relaxation of the deformation substructure. While precipitation leads to higher strength and homogenises deformation, improving ductility, substructure recovery may produce softening, but allow increased work hardening and improve ductility.

2. Experimental

The material used for study was a Cu-1%Cr-0.1%Zr alloy (by weight) supplied as round bar by Goodfellow. Cylinders of diameter 20 mm and length 60-80 mm were machined from this bar for ECAP processing and given a solutionising treatment of 980ºC for 1 h, in air, before water quenching. The solutionising treatment dissolves most of the Cr (and the Zr) but leave a small amount undissolved [16,17]. Undissolved Cr remains as coarse, widely spaced particles which are not expected to play any significant role in modifying behaviour during ECAP or affecting mechanical properties. Ageing treatments of 0.5-1 h at 450-500ºC were given to some samples before ECAP, and to others after ECAP, following a preliminary age-hardening study to determine suitable ageing conditions. ECAP processing was carried out, using the so-called route A, at room temperature for up to 12 passes through a circular cross-section die with die angle of 118º producing a true strain of 0.7 per pass, and using a speed of 20 mm/min.

Mechanical properties were evaluated by tensile testing, on samples with cylindrical gauges of diameter 3 mm and length 20 mm, with cylinder axis parallel to the pressing direction, at a nominal strain rate of 4 x 10^{-4}/s. Two samples were tested for each material condition, confirming excellent reproducibility of both strength and elongation. Disks for microstructural examinations were prepared by mechanical or electro-polishing in a direction perpendicular to the pressing inlet and exit directions. Mechanical polishing, using up to ¼ μm diamond abrasive and finally silica gel, was used to prepare samples for scanning electron microscopy (SEM), in back-scattered electron (BSE) mode, and electron-back-scatter-diffraction (EBSD). Electropolishing using a twin jet apparatus, with a mixture of 30% nitric acid and methanol at -15ºC and 15 V, was used to prepare samples for transmission electron microscopy (TEM). SEM examinations were carried out using a JEOL 6500 F instrument, equipped with an EBSD system using HKL Channel 5 software, and a Hitachi S-4800 instrument, both equipped with field-emission tips, and TEM studies using a JEOL 2010 FX instrument.

The deformation subgrain/grain substructure was quantified from the SEM-BSE micrographs, as well as from EBSD orientation maps. The SEM-BSE images were analysed at a magnification of 20,000 covering a total area of several hundred square microns, and several thousand subgrains/grains, using Sigma Scan Pro and Excel softwares. EBSD orientation maps were obtained over an area of several hundred square microns using a step size of 70 nm, examining several scans for each sample. The small step size was necessary to obtain good statistics of microstructure size and boundary misorientation in view of the fine deformation subgrain/grain structure. Dislocation cell

and subgrain microstructures were examined in TEM Bright Field images obtained with

diffraction contrast, and precipitates examined, also in TEM Bright Field images, under

phase contrast. Precipitate sizes and numbers were determined using the Sigma Scan

Pro and Excel software as above and foil thickness estimated from the number of

thickness fringes found at nearby grain boundaries. Particle numbers per unit volume

were also deduced by considering that the volume fraction of precipitate phase should

be that given by the equilibrium diagram for the corresponding ageing condition [16,17]

(considering that solubility varies with temperature as expected for an ideal solution).

3. Results

3.1. Preliminary age-hardening measurements

A short study of the age hardening behaviour was carried out to define suitable heat

treatments for ageing before and after ECAP. Hardness evolution is shown in Figure 1,

for solutionised material and after 4-8 ECAP passes. The solutionised material hardens

significantly after annealing for 30 mins at temperatures above 300ºC, Fig. 1a, reaching

a maximum after annealing for 0.5-1 h at 450-500ºC. The material is much harder after

ECAP, Fig. 1a, showing similar age hardening kinetics to reach higher hardness. There

is a slight acceleration of hardening kinetics relative to the solutionised material, which

is hardly as significant as suggested previously [9,12], and overage-softening appears on

annealing at 600ºC, which is not seen for solutionised material. Annealing at 450-500ºC

for 0.5-1 h led to the maximum hardness with little under or over-ageing, Fig. 1b. Based

on these studies, ageing treatments of 1-2 h at 450ºC and 0.5-1 h at 500ºC were selected

as suitable heat treatments for the evaluation of solutionised and ECAP material.

3.2. Mechanical behaviour of ECAP processed samples

Samples showed greatly increased strength after ECAP, with a rounded yield stage,

high work hardening to strains of 1-2%, and a long period of slowly reducing stress to

failure, as illustrated in Figure 2. These curves are similar to those reported before for

Cu-Cr, Cu-Cr-Zr [9-12] and other alloys [5]. Increasing ECAP strain led to a steady

increase in strength but little other change. Ageing at 450-500ºC after ECAP led to the

appearance of a yield discontinuity, see Fig. 2, followed by a short plateau of constant

stress, after which the stress fell slowly. Materials aged before ECAP showed stress-

strain curves similar to those of solutionised-ECAP material, see Fig. 2. The samples all

failed in a ductile manner with the formation of a neck and dimpled fracture surface.

Changes of yield stress with ECAP strain are shown in Figure 3 and Table 1, with the

effect of subsequent ageing (on solutionised material as well as material after ECAP)

also shown. Following ECAP, even with mild ageing (at 450-500ºC), there is little

difference (about 5-10 MPa) between yield and maximum stress. The first ECAP passes

lead to significant hardening with strength, thereafter, continuing to increase to the

highest strain level examined. Ageing the solutionised material leads to a large strength

increase, but a much smaller increase is seen after prior ECAP. The magnitude of the

age hardening is very similar (80 MPa) for all the ECAP material, irrespective of the

number of passes given. Of interest, the samples aged before ECAP show significantly

higher strengths (by about 40 MPa) than the corresponding ECAP+aged materials.

The evolution of tensile ductility with heat treatments and ECAP is summarised in

Table 1. The ductility falls from about 50% for solutionised material to near 10% after

ECAP, with little influence of the number of ECAP passes. While age hardening of solutionised material reduces ductility, the same treatment after ECAP leads to a slight increase in ductility from that of the deformed state. Materials given ageing treatments before ECAP show similar levels of ductility to solutionised and deformed materials. As seen in Fig. 2, the strain to maximum stress is typically about one tenth of the failure ductility, and varies with processing method in a similar way to the fracture strain.

3.3. Microstructure evolution during ECAP processing and annealing

Typical microstructures produced by ECAP and subsequent annealing are shown in Figure 4. A very fine substructure is seen, Fig. 4a, with some tendency to elongation near to the ECAP outlet direction, especially after few ECAP passes, tending to become more equiaxed after more passes, Figs. 4b. Occasional large (0.5 μm) Cr particles, undissolved during the solutionising treatment, were found for all materials. These were unaffected by deformation and were too widely separated to play any significant role in affecting the refinement of substructure. Some sub-boundaries show large contrast changes, indicative of large misorientations across the boundary, while others show much smaller contrast changes. In order to ensure reasonable quantification of substructure size for different materials, efforts were made to ensure similar levels of contrast for all micrographs and similar contrast detection resolution for all images analysed. The annealing treatments led to little noticeable change of substructure, see Fig. 4c, with materials aged prior to ECAP also showing very similar microstructures.

Microstructures of some materials were also examined using EBSD, illustrated in Figure 5. Fig. 5a shows an inverse pole figure map for material given 4 ECAP passes, where a slightly elongated microstructure is seen, similar to the SEM-BSE images in

Figs. 4. Boundaries of different misorientations are marked in Fig. 5a (black for high-angle boundaries, and white for low-angle boundaries) and a wide spread of boundary angles is confirmed. Fig. 5b shows a histogram of boundary misorientations measured from such maps, confirming that the vast majority of boundaries were low angle sub-boundaries with misorientation below 10º. A comparison of substructure size, measured from images such as that of Fig. 5a, confirms that the SEM-BSE images detect subgrains with misorientations down to 2º, close to the resolution of the EBSD technique. SEM-BSE images were thereafter used to characterise microstructure in view of the better quantification statistics possible using this method.

Histograms showing the distribution of subgrain size determined from SEM-BSE images are presented in Figure 6. In all cases the distribution shows a tail to higher subgrain size, with a maximum about three times the average, and mode value about 10% smaller than the average. The average value was thereafter taken to characterise the material. Fig. 6 illustrates the large reduction of subgrain size after 4 ECAP passes, which refines even more with additional ECAP passes. Annealing after ECAP leads to a slight increase in subgrain size, while annealing before ECAP results in material with significantly finer subgrain size. These variations are seen in Figure 7 and in Table 1, summarising the changes of subgrain size produced by different processing methods.

Typical microstructures seen by TEM are illustrated in Figure 8. The substructures are similar to those determined by SEM-BSE and EBSD – namely a slightly elongated subgrain substructure following 4 ECAP passes, and more equiaxed morphology after 8-12 passes, Fig. 8a-b, with very little change during short anneals, Fig. 8c. The TEM

images confirm the variability of boundary structures, with sharp boundaries of large

misorientation seen as well as dislocation cell boundaries of low misorientation. The

higher magnification image, Fig. 8b, shows many dislocations both inside subgrains as

well as at subgrain boundaries. Examination at high magnification and imaging under

conditions avoiding diffraction contrast showed that fine precipitates were formed in all

the annealed materials, whether annealed before or after ECAP, Figure 9. Such images

were obtained using phase contrast to visualise all precipitates present, avoiding the

overwhelming contrast of the many dislocations when imaging using diffraction

contrast. It is expected that phase contrast imaging will detect all particles present,

avoiding the selective imaging of only some of the particles when imaging in dark field

using diffracted beams of the precipitate phase. These images show a large number of

very fine precipitates, after the short heat treatments, with a few larger particles (up to

20-30 nm) which may have formed on pre-existing dislocations or sub-boundaries.

While no analysis has been carried out here, the fine particles are expected to be

coherent Cr precipitates while the coarser ones may be the same phase or Cu_4Zr, as

discussed elsewhere [1]. Figure 10 shows size distributions of precipitates determined

from these TEM images, with a large number of particles of size about 2 to 6 nm and a

few particles in the 10-25 nm range. Of special interest in Fig. 10 is the finer average

particle size determined in aged+ECAP material, compared with ECAP+aged material.

4. Discussion

4.1. Hardening due to ageing after severe plastic deformation

The variation of flow stress with processing condition will be examined using a Hall-

Petch type approach to relate strength to grain size, as well as to examine differences

brought about by annealing for precipitation, whether annealing is given before or after

ECAP. The justification of the Hall-Petch analysis, relating strength to subgrain size,

will be examined later.

Figure 11a shows experimental strength data, for initially solutionised material, as well

as material subsequently aged at 450-500ºC, and also material receiving such annealing

before ECAP processing, in relation to the square root of the measured subgrain size.

Following ageing after ECAP deformation, there is a notable strength increase relative

to the as-deformed strength. The data for such deformed+annealed material can be seen

to be related to the reciprocal square root of the grain size by exactly the same Hall-

Petch slope as for as-deformed materials. During these anneals there are only slight

increases in subgrain size (see Table 1 and Fig. 7, and compare Figs. 4a and c and also

Figs. 8a and c), which are in any case taken into account by the Hall-Petch analysis. The

ageing treatments given lead to a strength increase of about 100 MPa above that of the

as-deformed material, much less than the corresponding increase (about 200 MPa)

observed on annealing the solutionised material (see Figs. 3 and 11, and Table 1, as well

as the age hardening data of Fig. 1b).

It seems unlikely that precipitation in previously deformed material should be less fine

and produce less strengthening than when ageing solutionised material. A smaller

degree of hardening on ageing pre-deformed Cu-Cr alloy was also reported by Gao et al

[4], who noted the onset of recrystallization when annealing heavily deformed material

at high temperatures and long times. The microstructural studies carried out here,

however, confirm that there was no sign of recrystallization during the mild anneals

considered and the relatively small age hardening observed is presumably due to the counter-acting effects of precipitation hardening and dislocation recovery.

This conclusion is supported by a comparison of the precipitates formed after ageing of simply solutionised and of previously ECAP-deformed material. Examination by TEM of solutionised material aged for ½-1 h at 450-500ºC and material given the same treatments after previous deformation by 4 ECAP passes shows essentially identical precipitate sizes. Furthermore, estimations of the strengthening contribution of such precipitates confirm that they are indeed capable of producing the same hardening as found on ageing the solutionised material. The Orowan equation may be used to describe such strengthening, $\Delta\sigma_{OR}$, based on the particle size, ϕ, and the volume fraction of precipitate phase, f, as [18,19]:

$$\Delta\sigma_{OR} = M \, 2 \, G \, b \, / \{1.18 \, 4 \, \pi \, (\lambda - \phi)\} \, \ln(\phi/2b)$$

$$(1)$$

where λ is the spacing between particles on the slip plane, deduced from the particle size and volume fraction of precipitate as $\lambda = \phi/\sqrt{f}$. M is the Taylor factor (3), G the shear modulus of Cu (45 GPa) and b the Burgers vector (0.256nm). Using the mode particle sizes determined after annealing solutionised or pre-deformed material (such as in Fig. 10b), namely about 4.5-5.2 nm, and considering a precipitate volume fraction of about 0.61%, based on the solubility of Cr in Cu at the solutionising and ageing temperatures [16,17], the hardening contribution due to the precipitates is calculated as 170-200 MPa.

The observed hardening of only 100 MPa on ageing following ECAP, see Fig. 11a, is believed to be the consequence of two competing contributions – a precipitate hardening of 170-200 MPa (the same as for solutionised material) and a dislocation recovery softening of magnitude 70-100 MPa. The softening occurring is represented in Fig. 11b by the two Hall-Petch lines showing the experimental flow stress ($\sigma_{0.2}$) of the initially solutionised materials, and the experimental stress minus calculated precipitate strengthening ($\sigma_{0.2}$-σ_p) for these materials after subsequent ageing. In this case the Orowan strengthening deduced from equation (1) is used for the precipitate strengthening. Parallel lines are seen (of same Hall-Petch slope) with the line representing the aged material displaced down by about 70 MPa. Such softening is not due to differences of precipitation nor changes of subgrain size, but is expected to be caused by a reduction of dislocation density either within the subgrains or at the subgrain boundaries. There is little clear evidence in the present study of such changes of dislocation density or of boundary misorientation on annealing but any possible reduction of dislocation density inside subgrains or at subboundaries requires detailed examination by TEM that is beyond the scope of the present study.

4.2. Strength of material aged before severe plastic deformation

Ageing of material (for 1 h at 450/500ºC) to peak hardness before processing by ECAP has led to material with a finer grain size, see Fig. 7, and very high level of strength (see Fig. 3). Such ageing is expected to produce precipitates of size about 5 nm (similar to those of Figs. 9b and 10b), although following ECAP their size was shown to have been reduced to about 3 nm (Figs. 9a and 10a). The presence of the fine Cr precipitates, instead of Cr in solid solution, has led to greater microstructural refinement occurring during ECAP. Cr particles, with an initial size of 5 nm, are clearly better at restricting

dislocation motion and recovery during deformation than Cr in solid solution. Cr is

known to produce weak solution hardening in Cu, in contrast with other cases, such as

Mg in Al, which are known to produce strong solution hardening [20,21]. It is also clear

that many of the Cr particles have been sheared to finer size during ECAP processing,

and possibly some have redissolved. It is, however, difficult to determine volume

fraction of the precipitate phase with sufficient precision to confirm this possibility.

The strength of materials where precipitation took place before ECAP deformation may

be examined in terms of grain size refinement using the Hall-Petch plot of Fig. 11. It is

clear here that most of the higher strength achieved is due to the greater refinement of

microstructure with pre-existing particles. As seen in Fig. 11a, however, there appears

to be an additional strengthening component, of the order of 30-50 MPa in addition to

Hall-Petch strengthening. This strengthening is presumably caused by the precipitates

that remain, which have reduced in size from the initial 5 nm to the 2.5-3 nm found after

ECAP, see Figs. 9 and 10. Such small precipitates are unlikely to interact with

dislocations by the Orowan mechanism, and an alternative approach based on shearing

of fine particles may be considered. Strengthening, $\Delta\sigma_p$, may now be written [22] as:

$$\Delta\sigma_P = M \ \beta \ [G_F|\epsilon|]^{3/2} \ [f \ r \ b/2 \ S]^{1/2} \qquad (5)$$

Here β is a constant (3.5), G_F the shear modulus along the slip plane in the slip direction

(30 GPa), ϵ the constrained misfit of the particle in the matrix (1.6×10^{-2}), r the particle

radius, S the dislocation line tension ($Gb^2 \approx 2 \times 10^{-9}$ N), with other terms having the

meanings and values defined previously. Using this expression, the strengthening due to

particles of size 2.5-3 nm is estimated as 75-85 MPa, somewhat less if the precipitates

are considered to have partially dissolved during ECAP deformation, in reasonably

good agreement with the observed particle strengthening contribution (30-50 MPa). In Fig. 11b are shown the data points corresponding to the materials annealed for precipitation before ECAP after removing a particle strengthening contribution taken to be about 30-50 MPa. The strength data then fall on exactly the same Hall-Petch line corresponding to the deformed as-solutionised material, confirming an identical strengthening effect of the fine subgrain microstructure.

4.3. Hardening due to severe plastic deformation of solutionised material

Strengthening on ECAP processing of solutionised material may be examined in terms of microstructural refinement by considering grain size reduction. Strength may be related to the reciprocal square root of the measured subgrain size using the standard Hall-Petch approach shown in Figure 11. The Hall-Petch line shown here essentially connects the undeformed state with the three deformed states after 4, 8 and 12 ECAP passes, with the grain size variation between these being too small to establish any dependence based on these three states alone. As such, this analysis remains somewhat uncertain and speculative. Strength after ECAP may be reasonably well related to the undeformed, large grained material in terms of a Hall-Petch dependence with a matrix term (σ_0) of 84 MPa and a Hall-Petch slope (k_{HP}) of 129 MPa$\sqrt{\mu m}$. σ_0 represents the strength of single crystal solid solution and k_{HP} the strengthening effect of the grain boundary. The value of k_{HP} is essentially identical to that suggested by Hansen [23] for Cu, giving good support to the present analysis. It may be noted at this time that the small amount of coarse Cr particles in these materials was too widely separated to play any significant role in modifying substructure or in strengthening (an Orowan strength of about 10 MPa was estimated). These coarse particles remain unaffected by any

deformation or ageing treatment, and will not influence the present study examining the

role of heavy deformation, with any prior or subsequent ageing treatments.

The analysis above considers that all boundaries detected, with misorientations of 2º

and greater, can be treated as high-angle grain boundaries in respect to strengthening.

An alternative approach, based on studies of Kuhlmann-Wilsdorf [24-26], considers that

the subboundaries may be considered as constituting a high density of dislocations,

depending on the subgrain size, which produces Taylor hardening. According to

Kuhlmann-Wilsdorf [24], this strengthening ($\Delta\sigma_\rho$) can be written as:

$$\Delta\sigma_\rho = M\ \alpha\ G\ b\ \sqrt{\rho} \tag{3}$$

where α is a constant of magnitude 0.4 [26], ρ the dislocation density, with the other

terms defined before. Considering that the average spacing between dislocations ($1/\sqrt{\rho}$),

which are mostly contained in the cell walls, can be related to the cell size D_c by a

constant K of value about 10 [24-26], we can describe dislocation cell hardening

($\Delta\sigma_{Dc}$):

$$\Delta\sigma_{Dc} = M\ \alpha\ G\ b\ K/D_c \tag{4}$$

This approach, however, predicts strengthening many times greater than is observed.

Yet another approach [23] considers the same Taylor hardening by the dislocations of

the subgrain boundaries, but takes account of the variation of dislocation density with

both subgrain size and with boundary misorientation θ. Equation (3) is rewritten,

considering the subgrain boundary area per volume of material to be about 3/D and the

dislocation density per boundary area to be related to the misorientation as θ/b. The value of cell/subgrain strengthening ($\Delta\sigma_D$) is then written as:

$$\Delta\sigma_D = M \, \alpha \, G\sqrt{(3 \, \theta \, b/D)} \tag{5}$$

This equation predicts a strength dependence on reciprocal square root of the subgrain size, identical to the Hall-Petch analysis. The proportionality between strengthening and reciprocal square root of subgrain size (equivalent to k_{HP}) is predicted to be about 220 MPa√μm for a typical boundary misorientation of 2º and the experimentally observed value (129 MPa√μm) is deduced only for an unrealistically small average boundary misorientation: this approach thus also predicts excessively high strengthening.

In conclusion, and even though the range of experimental variation of strength and subgrain size is narrow for the range of processing conditions examined, the strengthening produced by ECAP processing of solutionised material appears consistent with the Hall-Petch model, i.e. is due to the refinement of the subgrain size.

4.4. Influence of processing conditions on tensile ductility

The large fall in ductility observed after severe plastic deformation may be understood as the exhaustion of work hardening capacity by heavy deformation which means that the maximum stress is quickly reached on tensile testing with resistance to necking and failure leading to a relatively large fracture ductility (about 10%). Mild anneals for precipitation after ECAP lead to small increases in ductility (to 11-12%) while similar annealing for precipitation prior to ECAP leaves to the initial moderate ductility (about 10%). The improved ductility by annealing after ECAP appears to be due to dislocation

recovery processes and does not seem to be due to the presence of the fine precipitates.

Further work is required to understand these small changes with processing condition.

5. Summary

ECAP carried out using up to 12 passes, imposing strains greater than 8, leads to significant hardening of the Cu-Cr-Zr alloy studied, albeit with a large reduction of ductility. The increased strength can be well explained using the concept of Hall-Petch strengthening due to the many grain/subgrain boundaries rather than by dislocation hardening. The fall in ductility is caused by the loss of work hardening capacity after imposing high levels of strain.

Mild annealing treatments (1/2-1 h at 450-500ºC) lead to the appearance of precipitates as well as slight coarsening of the subgrain structure produced by ECAP straining. The age hardening due to precipitate formation is partially countered by dislocation recovery-softening inside the subgrains or at the subgrain boundaries.

The equivalent heat treatments carried out for precipitation prior to ECAP processing lead to increased strength levels due to the greater refinement of subgrain size as a consequence of particle-dislocation interactions. At the same time, the particles are somewhat sheared to finer sizes, possibly being partially but not completely dissolved.

Changes of ductility according to processing condition are shown to be due to the extent of dislocation accumulation or recovery during processing, with no evidence of a direct influence of the precipitate particles themselves.

Acknowledgements

References

[1]   D.J. Edwards, B.N. Singh and S. Tahtinen, J. Nucl. Mater. 367-370 (2007) 904.

[2]   F. Huang, J. Ma, H. Ning, Z. Geng, C. Lu, S. Guo, X. Yu, T. Wang, H. Li and H. Lou, Scripta Mater. 48 (2993) 97.

[3]   H. Dybiec, Z. Rdzawski and M. Richert, Mater. Sci. Eng. A108 (1989) 97.

[4]   N. Gao, E. Huttunen-Saarivirta, T. Tianen and M. Hemmila, Mater. Sci. Eng. A342 (2003) 270.

[5]   R.Z. Valiev and T.G. Langdon, Prog. Mater. Sci. 51 (2006) 881.

[6]   A.P. Zhilyaev and T.G. Langdon, Prog. Mater. Sci. 53 (2008) 893.

[7]   M.H. Shih, C.Y. Yu, P.W. Kao and C.P. Chang, Scripta Mater. 45 (2001) 793.

[8]   A. Mishra, B.K. Kad, F. Gregori and M.A. Meyers, Acta Mater. 55 (2007) 13.

[9]   A. Vinogradov, T. Ishida, K. Kitagawa and V.I. Kopylov, Acta Mater. 53 (2005) 2181.

[10]   C.Z. Xu, Q.J. Wang, M.S. Zheng, J.W. Zhu, J.D. Li, M.Q. Huang, Q.M. Jia and Z.Z. Du, Mater. Sci. Eng. A459 (2007) 303.

[11]   K.X. Wei, W. Wei, F. Wang, Q.B. Du, I.V. Alexandrov and J. Hu, Mater. Sci. Eng. A528 (2011) 1478.

[12]   A. Vinogradov, V. Patlan, Y. Suzuki, K. Kitagawa and V.I. Kopylov, Acta Mater. 50 (2002) 1639.

[13]   N. Takata, Y. Ohtake, K. Kita, K. Kitagawa and N. Tsuji, Scripta Mater. 60 (2009) 590.

[14]   R.K. Islamgaliev, N.F. Yunusova, I.N. Sabirov, A.V. Sergueeva and R.Z. Valiev, Mater. Sci. Eng. A319-321 (2001) 877.

[15]   Z. Horita, K. Ohashi, T. Fujita, K. Kaneto and T.G. Langdon, Adv. Mater. 17 (2005) 1599.

[16]   N. Saunders, Mater. Sci. Technol. 3 (1987) 671.

[17]   D.J. Chakrabarti and D.E. Laughlin, Bull. Alloy Phase Diagrams, 5 (1984) 59.

[18]   M.A. Morris and D.G. Morris, Acta Metall. 36 (1988) 1187.

[19]   D.G. Morris and M.A. Morris, Mater. Sci. Eng. 104A (1988) 201.

[20]   Y. Iwahashi, A. Horita, M. Nemoto and T.G. Langdon, Metall. Mater. Trans. 29A (1998) 2503.

[21]   D.G. Morris and M.A. Muñoz-Morris, Acta Mater. 50 (2002) 4047.

[22]   N. Buttner, K.-D. Fusenig and E. Nembach, Acta Metall. 35 (1987) 845.

[23]   N. Hansen, Scripta Mater. 51 (2004) 801.

[24]   D. Kuhlmann-Wilsdorf, Mater. Sci. Eng. 113A (1989) 1.

[25]   J. Weertman and J.R. Weertman, Mechanical properties, mildly temperature-dependent, in Physical Metallurgy, Eds. R.W. Cahn and P. Haasen, 3rd. edition, North-Hollnd Physics Publishing, Amsterdam (1983), p. 1259.

[26]   M. Sauzy and L.P. Kubin, Prog. Mater. Sci. 56 (2011) 725.

Table 1
Summary of materials examined, microstructure and mechanical properties

Material state	Yield Stress (MPa)	Tensile Stress (MPa)	Ductility (%)	Grain Size (nm)
Solutionised	101	229	50	60×10^3
Solutionised+450°C,1h	297	405	28	
Solutionised+500°C,1h	295			
4EpRT	429	434	9.2	144±12
8EpRT	455	460	10	114±12
12EpRT	478	490	10	110±12
4EpRT+450°C,1h	505	507	12	155±12
4EpRT+450°C,2h	500	500	11.2	245±12
4EpRT+500°C,0.5h	483	488	9.6	190±12
8EpRT+450°C,1h	537	540	11	135±12
12EpRT+450°C,1h	563	563	9	118±12
450°C,1h+4EpRT	532	539	9.2	100±12
500°C,1h+4EpRT	540	543	8.6	85±12
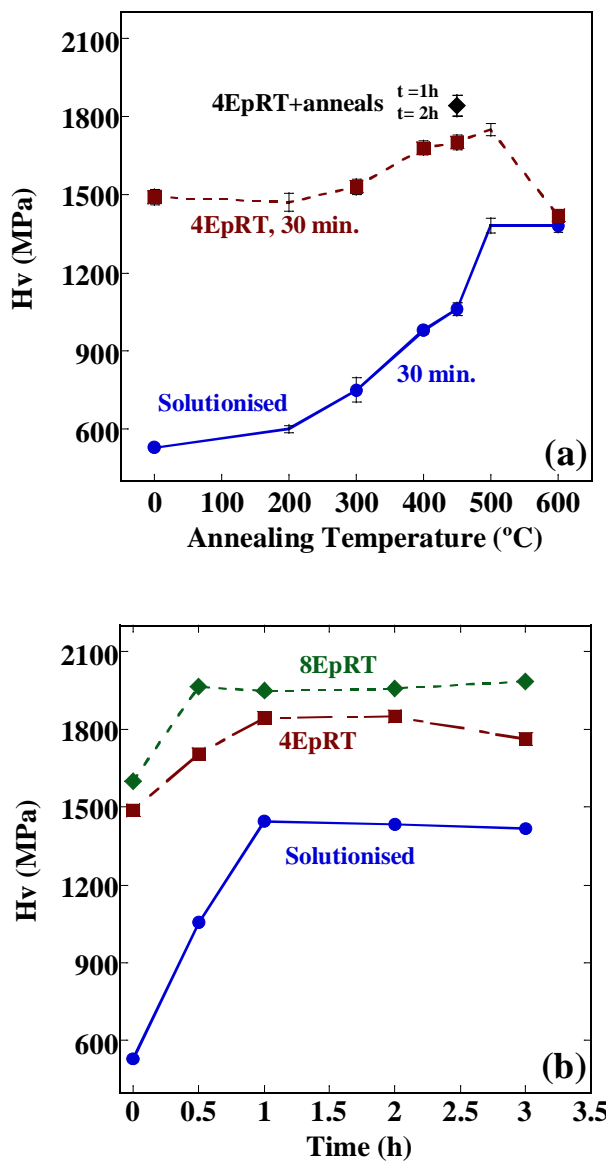
Figure 1:   Evolution of hardness of solutionised and ECAP material during subsequent annealing: (a) for materials annealed for 30 mins at each temperature (some annealed for 1 or 2 h); (b) for materials annealed at 450ºC for different times.
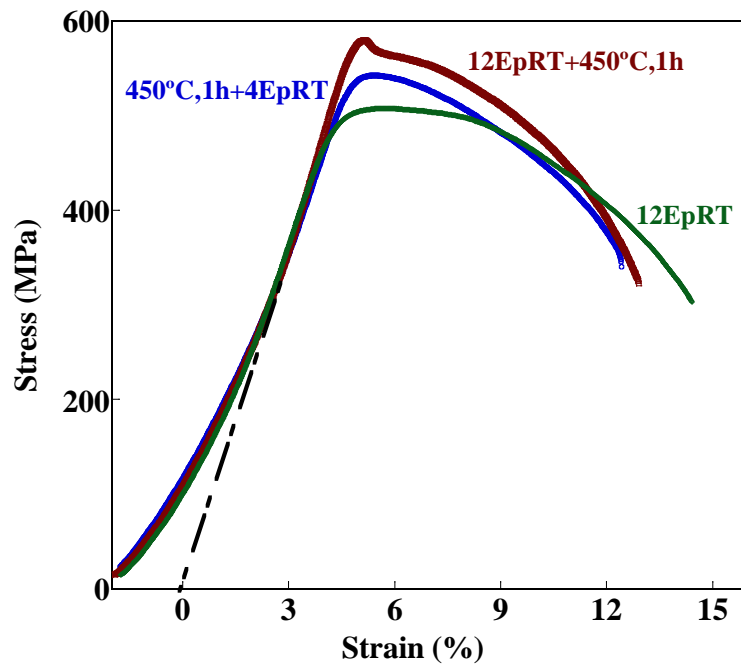
Figure 2:   Typical engineering stress-strain (crosshead displacement /sample gauge length) curves measured during tensile testing of several ECAP and annealed materials: after ECAP to 12 passes and subsequently annealed at 450ºC; and material annealed for 1 h at 450ºC and then given 4 ECAP passes.
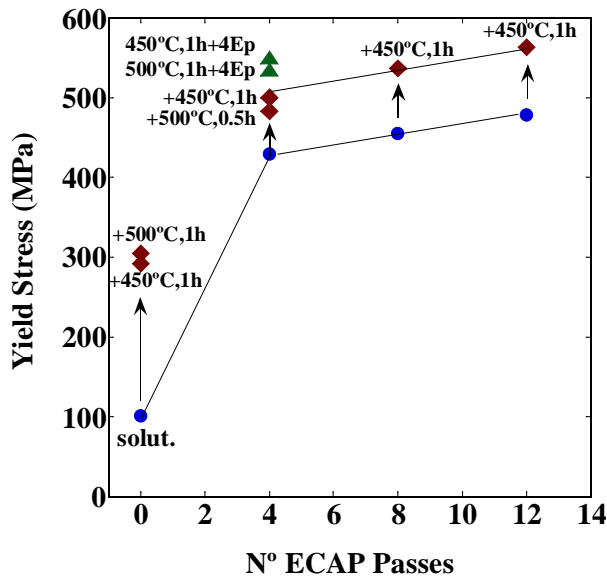
Figure 3: Evolution of yield stress with number of ECAP passes for initially solutionised (solut) material. The effect of subsequent ageing for 0.5-1 h at 450-500ºC is also shown. Data are also given for material aged at 450-500ºC for 1 h and subsequently given 4 ECAP passes.
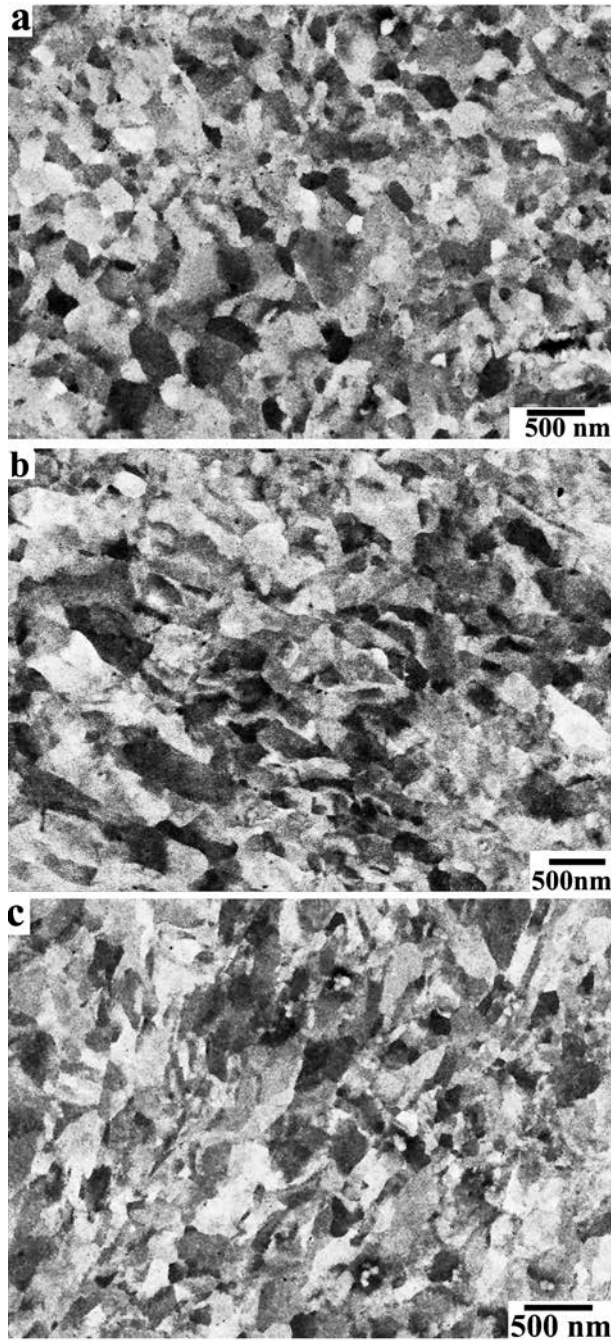
Figure 4:   SEM images in BSE contrast mode illustrating typical substructures found after processing solutionised material to: (a) 4 ECAP passes, (b) 12 ECAP passes, and (c) 4 ECAP passes and annealed for 1 h at 450ºC.
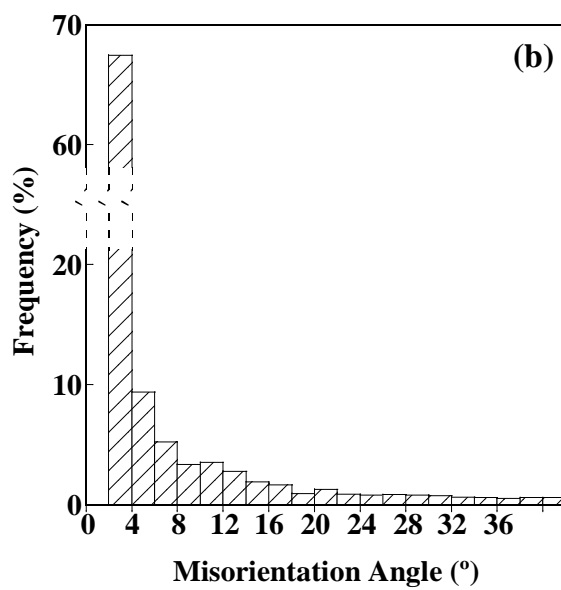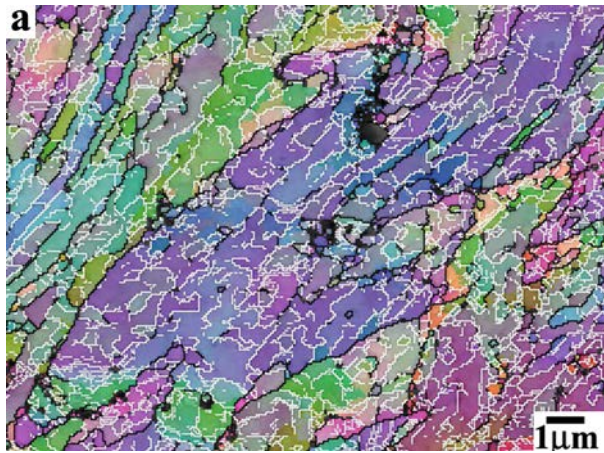
Figure 5:   (a) Inverse pole figure map of the transverse section through material given 4 ECAP passes. Grain orientations are coloured according to the usual unit triangle convention (001 – red; 011 – green; 111 – blue). High angle boundaries (misorientation above 15º) are indicated by black lines, and low angle boundaries (<2º misorientation) by white lines. (b) Histogram showing frequency of occurrence of boundary misorientations for material given 8 ECAP passes.
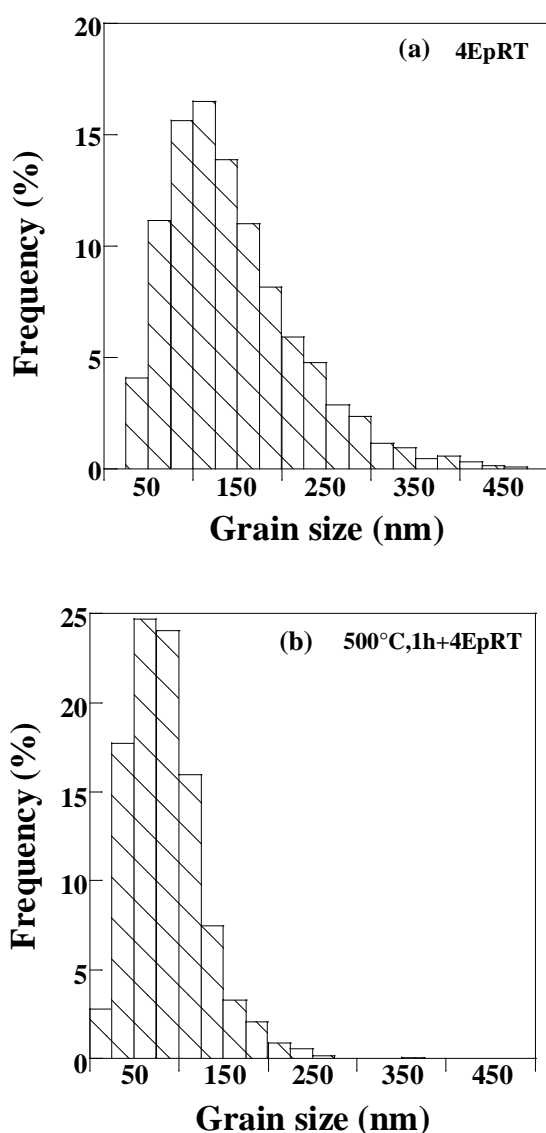
Figure 6:   Histograms showing distribution of subgrain size produced by ECAP with previous or subsequent anneals: (a) material given 4 ECAP passes; (b) material annealed 1 h at 500ºC before giving 4 ECAP passes; (c) material given 8 ECAP passes and subsequently annealed for 1 h at 450ºC.
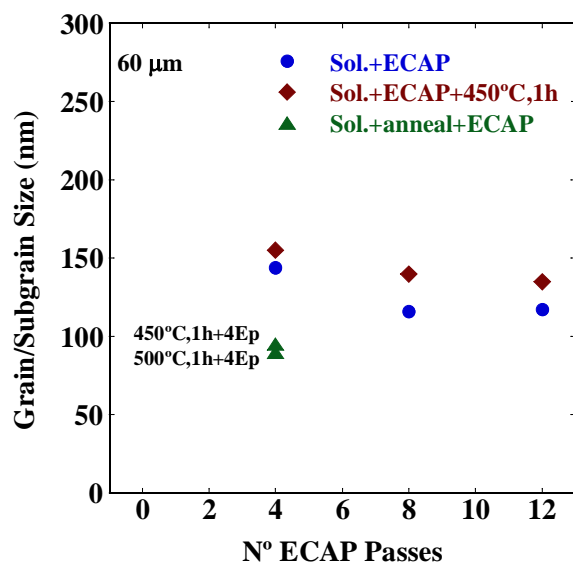
Figure 7: Variation of average subgrain size with processing conditions: material was initially solutionised (Sol) with a large grain size, then processed by ECAP. Materials were subsequently given an anneal at 450ºC. Some samples were annealed at 450-500ºC before receiving ECAP.
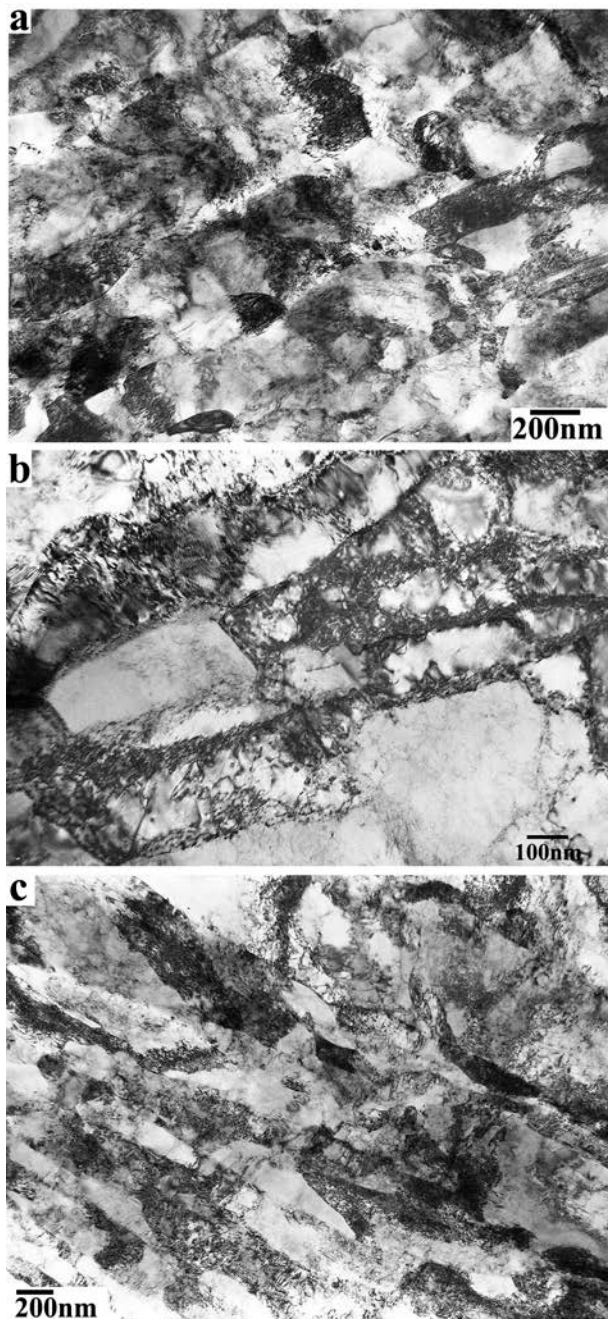
Figure 8:   Bright field TEM images showing deformation substructure in material after (a-b) 8 ECAP passes, and (c) 4 ECAP passes followed by an anneal of 1 h at 450ºC. (b) shows a higher magnification of (a) where high dislocation density is more clearly seen.
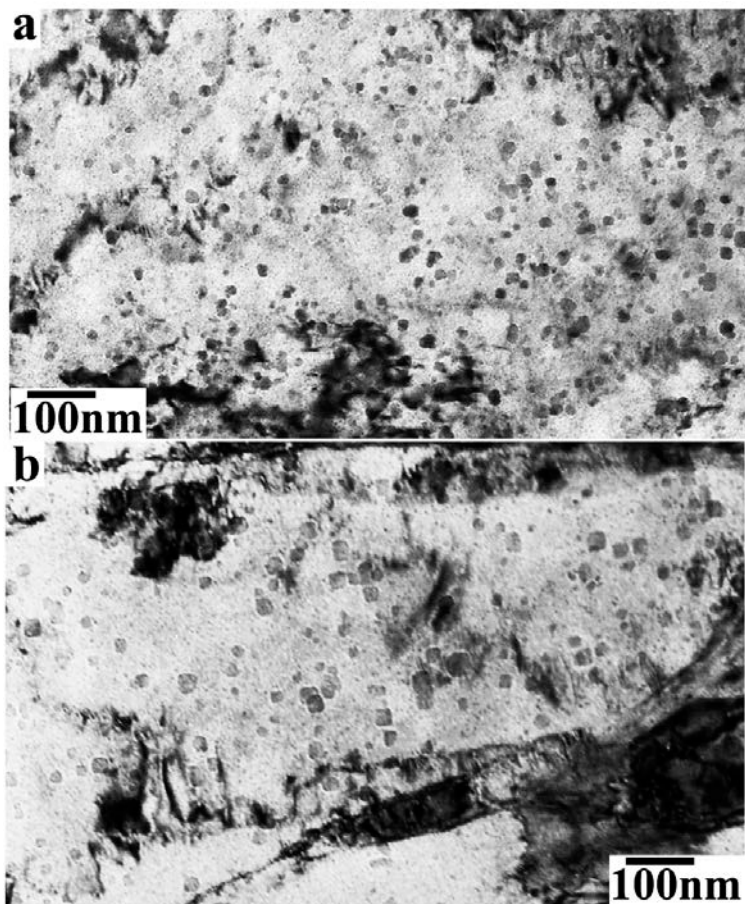
Figure 9:   Precipitates in material which has been heat treated as (a) annealed for 1 h at 500ºC before 4 ECAP passes, and (b) 4 ECAP passes followed by ½ h at 500ºC. Images were obtained under conditions with no diffraction contrast using phase contrast.
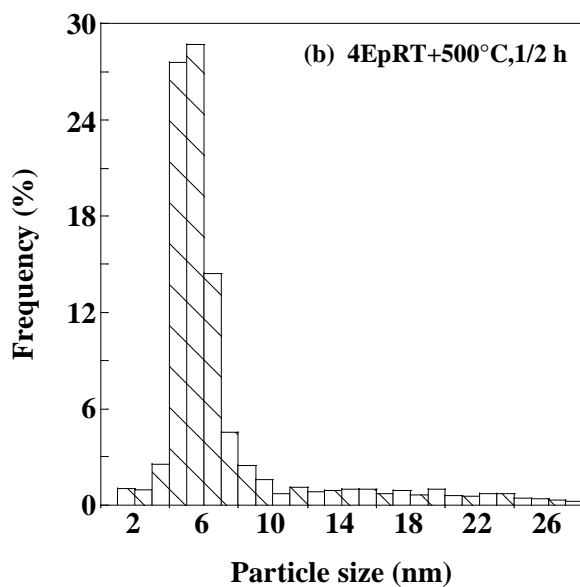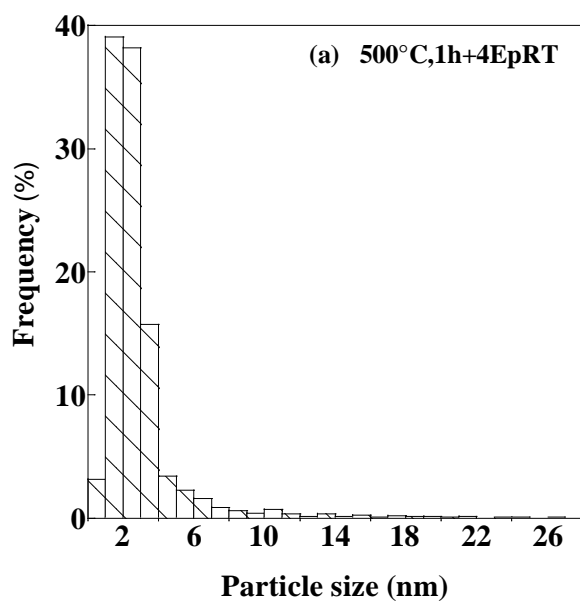
Figure 10: Histograms showing the distribution of precipitate size in (a) material annealed for 1 h at 500ºC and then given 4 ECAP passes, and (b) material given 4 ECAP passes before annealing ½ h at 500ºC.
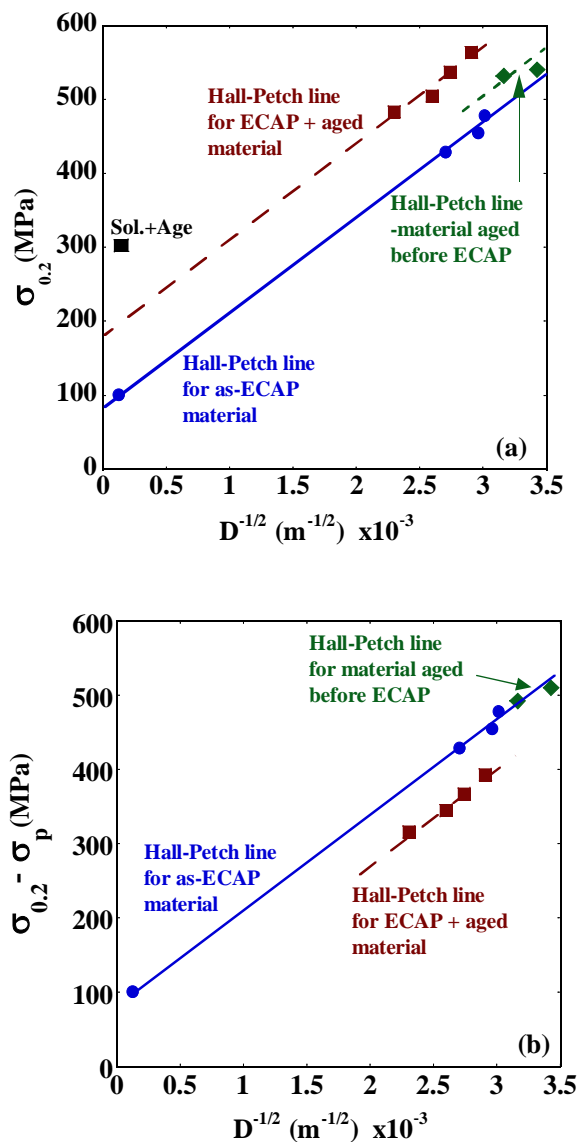
Figure 11: Hall-Petch representation of the strength of as-ECAP deformed material (after 4, 8 and 12 passes), relative to the strength of the initial, solutionised material, and also the same material after a subsequent age hardening treatment of 1 h at 450ºC. Strength of material age hardened for 1 h at 450ºC and 500ºC before 4 ECAP passes is also shown. (a) shows experimental yield strength data ($\sigma_{0.2}$) and (b) the same data after removing calculated values for precipitation hardening, as ($\sigma_{0.2} - \sigma_P$). See text for details.